



International Journal of Research in Academic World

Received: 25/May/2023

IJRAW: 2023; 2(6):64-71

Accepted: 29/June/2023

Non-Violating Unitarity Constraints in Extra Z' Heavy Particle Effect at Tesla Collider (CERN) CM Energy More than 500 GeV

*¹Dr. Ram Swaroop Sahu*¹Professor, Department of Physics, Government PG College, University of Rajasthan, Sambhar Lake, Jaipur, Rajasthan, India.

Abstract

We have done calculation for the unitarity delay. We have also wants to include very heavy particle which has been showed violating of unitarity as well as unitarity delay. We found that Föster limit has been explained and stopped the violation of unitarity and continue with the unitarity delay. It means that CM energies have very high energy more 3000 GeV the unitarity delay breakdown. Föster limit provides us that unitarity constraints obeys the law of unitarity delay. Our pervious calculation of S, T & U parameters results are very strong parameters for the physics beyond the SM. The radiative corrections of W^+ & W^- gauge boson through vertex of $Z_1 WW$, $Z_2 WW$ and $Y WW$ vertices we found the results are favour S, T and U parameters results. This calculation completes our research work to the cross- section and vertex corrections. We study the cross section that is non-delayed Unitarity violation. Can it stop violation? If we include heavy exotic lepton doublet $L = \begin{pmatrix} N \\ \nu_L \end{pmatrix}$ in the vertex diagram also.

Keywords: Föster limit, vertex, vertices, unitarity, delay unitarity

Introduction

Z' heavy particle effects $e^- e^+ \rightarrow W^- W^+$ [1, 2]

Radiative corrections allow us to probe the high-energy world with comparatively low-energy experiments. Because any intermediate state allowed by symmetry, however heavy (like Z', Higgs particles) can appear as a quantum fluctuation, precision experiments which isolate radiative corrections can probe for particles with masses much higher than the experimental energy scale. Now that we are entering the era of experiments on the properties of the weak vector bosons, it is interesting to think of precision experiments, which might be carried out on the new fundamental particles. Such experiments would necessarily be done at energies of 500 GeV or even much higher; still extending the reach of the available machine energy by the measurements sensitive to the radiative corrections is an attractive possibility [3]. We observe that in this research that even within the standard model or extra U (1) model the introduction of new heavy particles can cause large deviations from the tree-level cross-section. New species with perfectly conventional electroweak coupling naturally yield different radiative corrections to the s- and t-channel diagram involved in the tree-level unitarity cancellation. All these corrections together must sum to zero

(to leading order) for asymptotic. However, the regime of greatest experimental interest corresponds to the case of a state with mass M to large to allow its pair productions at the high-energy lepton collider: $s \leq M^2$, while $s \gg (m_w)^2$. In this regime, there is no reason for the Unitarity cancellations to occur, and indeed, we find enhanced radiative corrections of order $(\frac{s}{\pi m_W^2})$. These effects can be readily identified experimentally. We call this phenomenon in which heavy-particle radiative corrections postpone the asymptotic cancellation among diagrams, "Unitarity Delay" [1, 2].

Objective and General Formalism [3]

BPZH begins their analysis with a general parameterization of the WWA and WWZ vertices. Let f_i^V represent form factors (V=A or Z) and T represent canonical Lorentz structure (simplicity carrying three vector indices). The vertex shown in Fig. 1 is built from the ingredients as

$$\Gamma_V^{\alpha\beta\mu}(q, \bar{q}, p) = \sum_{i=1}^7 T_i f_i^V \quad (1)$$

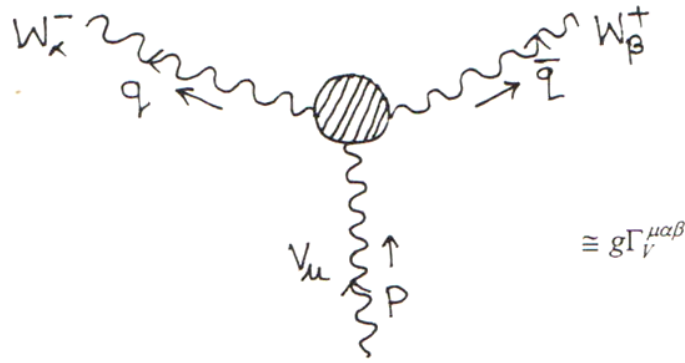


Fig 1: The general vertex for W pairs.

The form factors are dimensionless functions of s and m_w . We will consistently ignore the electron mass. Using eq.(1) we can write the full amplitude arising from the s-channel diagrams for $e^- e^+ \rightarrow W^- W^+$ as shown in Fig. 2(a):

$$M = ie^2 Q (\bar{v} \gamma_\mu u) \frac{1}{p^2} \Gamma_A^{\mu\alpha\beta} \epsilon_\alpha^*(q) \epsilon_\beta^*(\bar{q}) + ie^2 \frac{(I_3 - Q \sin^2 \theta_w)}{\sin^2 \theta_w} (\bar{v} \gamma_\mu u) \frac{1}{(p^2 + m_{Z_i}^2)} \Gamma_{Z_i}^{\mu\alpha\beta} \epsilon_\alpha^*(q) \epsilon_\beta^*(\bar{q}) \quad (2)$$

Where $Z_i = Z_{1, 2}$, $P^2 = -s$, u and v are electron and positron Dirac spinors and $\epsilon_\alpha^*(q)$, $\epsilon_\beta^*(\bar{q})$ are polarization vectors of W^\pm , respectively.

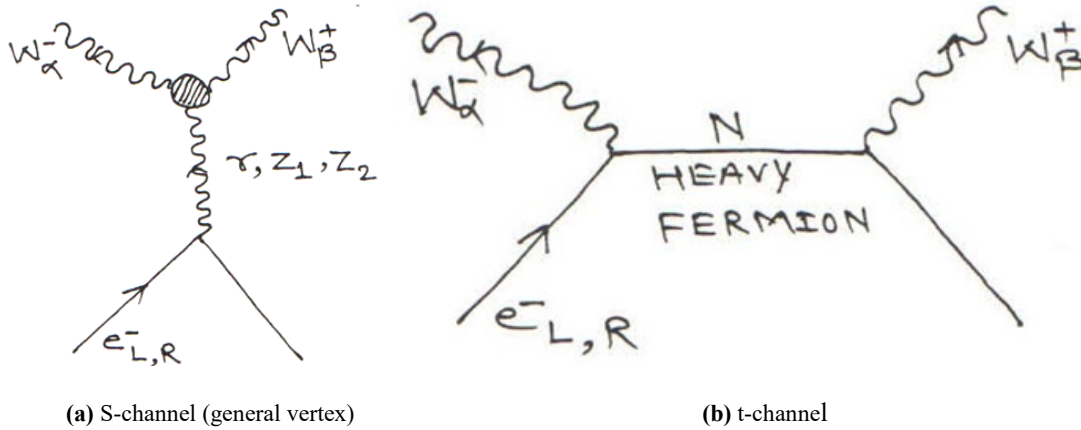


Fig 1 (a, b): The amplitude for $e^- e^+ \rightarrow W^- W^+$

We may consider the electron to have definite velocity and write $I_3 = -\frac{1}{2}$ for e_L , $I_3 = 0$ for e_R . Eq. (2) suggests that we combine the photon and Z or Z' vertices according to

$$F_i = Q f_i^A + \frac{(I_3 - Q \sin^2 \theta_w)}{\sin^2 \theta_w} \left(\frac{s}{s - m_{Z_i}^2} \right) f_i^{Z_i}, (i = 1, 2 \dots 7) \quad (3)$$

And define $\Gamma^{\mu\alpha\beta}$ as the vertex built from these form factors according to eq. (1)

$$\Gamma^{\mu\alpha\beta}(q, \bar{q}, p) = \sum_{i=1}^7 F_i T_i \quad (4)$$

The differential cross section for W^\pm scattering from electron and positron states of definite helicity into W states of definite polarization. Expressing these cross section in units of the point cross section $1R = \frac{4\pi\alpha^2}{3s}$

$$\frac{d\sigma}{d \cos\theta} = \frac{3}{8} \beta \Sigma(R) \quad (5)$$

Where $\beta = \sqrt{\left(\frac{1-4m_W^2}{s}\right)}$, β is W velocity.

Where θ is the scattering angle in the center of mass frame, and the subscripts T, L denote transverse and longitudinal polarization of the W^+ and W^- . For e_L^+ , e_R^- , we find the more complicated result in the form of amplitude A_1, A_2, A_3, A_4 and

$$A_5 = \beta \frac{s}{m_w^2} \left[\frac{1}{2} F_3 - \left(\frac{1}{2} - \frac{m_w^2}{2} \right) F_1 + \frac{1}{4} \beta^2 \frac{s}{m_w^2} F_2 + \frac{1}{4 \sin^2 \theta_w} + \frac{m_w^2}{s \beta^2 \sin^2 \theta_w} \left(1 - \frac{2m_w^2}{sD} \right) \right] \quad (6)$$

F_1, F_2, F_3 form factors.

For Factors pertaining to Z_2 [4]

We assume that the mass difference M_{H^\pm} and Z_2 is always small, which it is and set

$$\begin{aligned} \Delta m^2 &= [M_{H^\pm}^2 - M_{Z_2}^2], \\ m^2 &= \left[\frac{1}{2} (M_{H^\pm}^2 + M_{Z_2}^2) \right] \end{aligned} \quad (7)$$

With $\Delta m^2 \ll m^2$. Then for $m_w^2 < s \ll m^2$, we use directly the asymptotic repression for C_δ 's ($\delta = 0, 1, 2 \dots 7$) from qe.(16) of ref.[3]. On the other hand, when $s \gg m^2$, dropping $\frac{\Delta m^2}{m^2}$, we use the non-asymptotic expression for C_δ 's as given in qe.(17) of ref. [3]

Appendix

We calculated values of charged Higgs mass M_{H^\pm} and neutral Higgs mass M_{H^0} as a function of Z_2 and Θ_E using the top quark $m_t = 173.8 \pm 5.2$ GeV/c²[6] for the extra U(1) Superstring Inspired Model parameters [1,5].

Table 1: Charge Higgs mass M_{H^\pm} and Neutral Higgs mass M_{H^0} as function of Z_2 and θ_E .

S. No.	M_{Z_2} (GeV)	Θ_E (Radian)	M_{H^\pm} (GeV)	M_{H^0} (GeV)
1	555	-0.0097	476.21	702.94
2	565	-0.0093	485.68	715.65
3	575	-0.0090	495.00	728.35
4	585	-0.0087	504.28	741.06
5	595	-0.0084	513.61	753.77
6	605	-0.0081	522.93	766.48
7	615	-0.0078	532.24	779.18
8	620	-0.0077	536.89	785.54

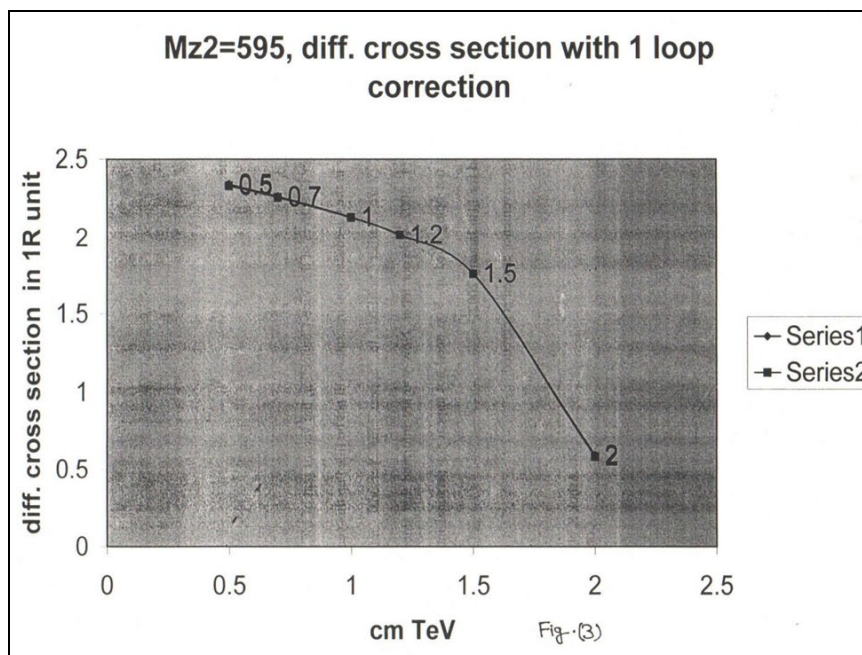


Fig 2: Differential cross section and cm energy at $= M_{Z_2}$ 595 Gev.

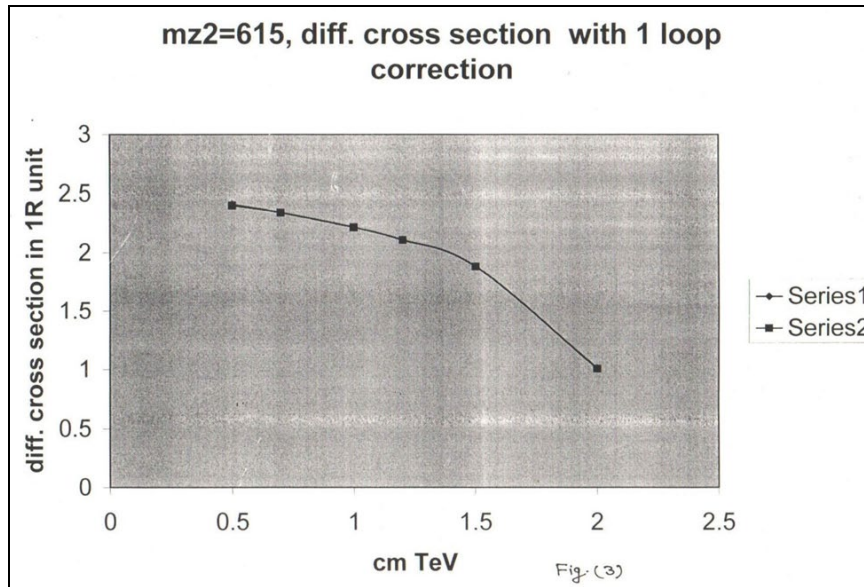


Fig 3: Differential cross section and cm energy at $M_{Z_2} = 615$ GeV.

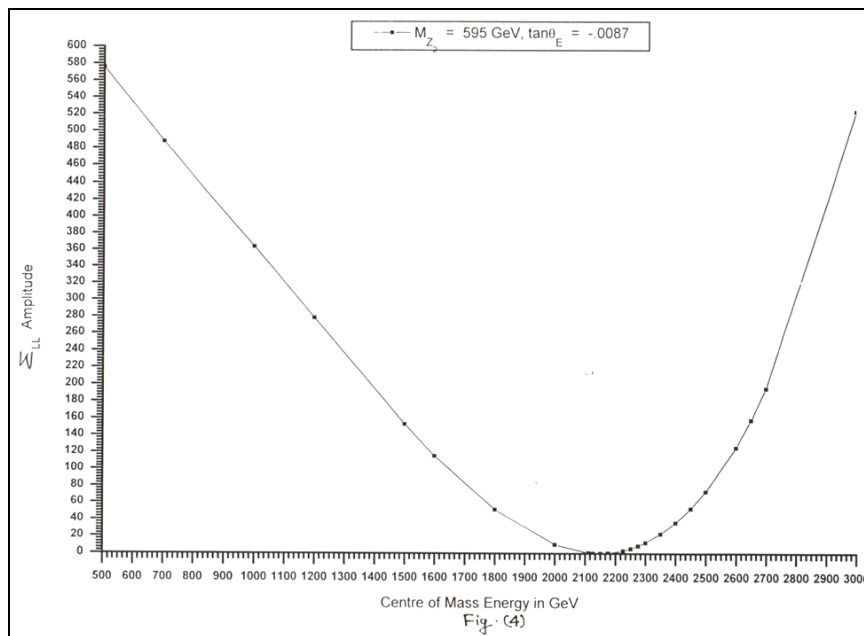


Fig 4: Σ_{LL} Amplitude and cm energy at $M_{Z_2} = 595$ GeV and $\tan \theta_E = -0.0087$.

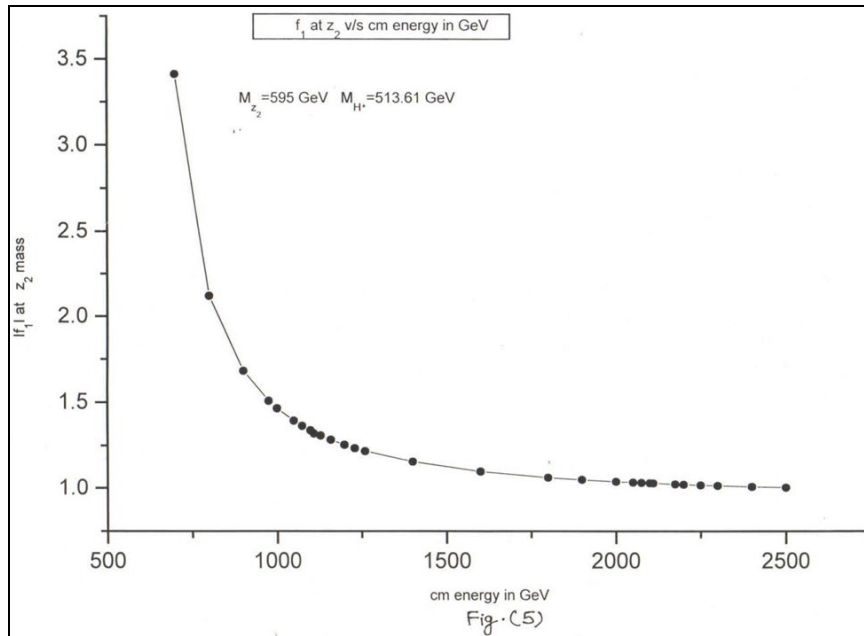


Fig 5: $|f_1|$ at Z_2 mass and cm energy at $M_{Z_2} = 595 \text{ GeV}$ and $M_{H^+} = 513.61 \text{ GeV}$.

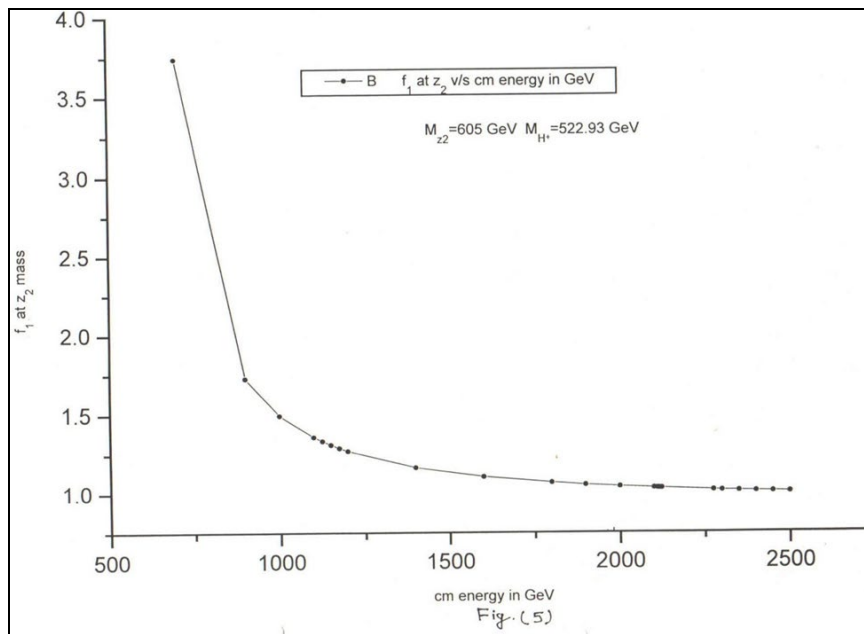


Fig 6: f_1 at Z_2 mass and cm energy at $M_{Z_2} = 605 \text{ GeV}$ and $M_{H^+} = 522.93 \text{ GeV}$.

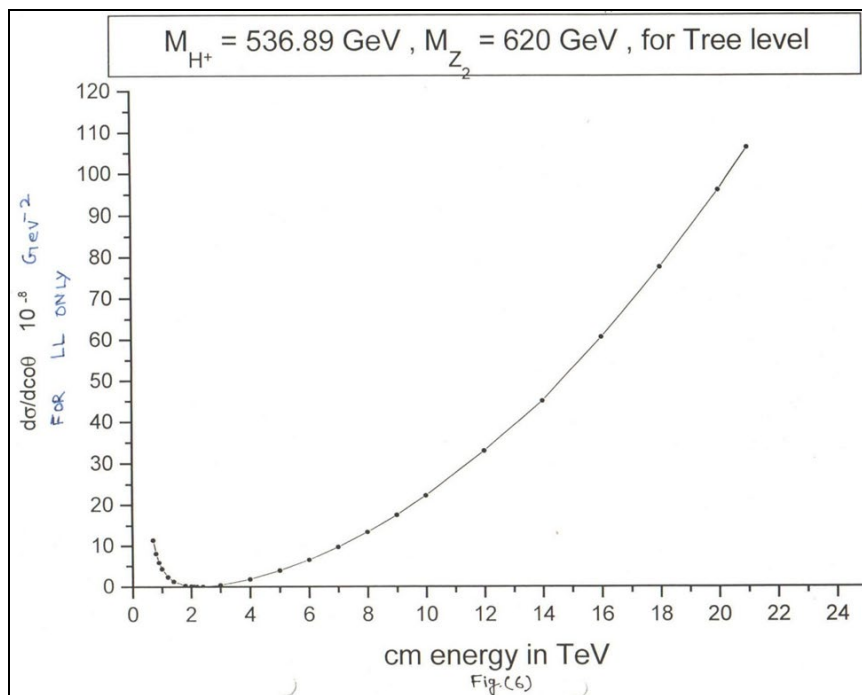


Fig 7: $\frac{d\sigma}{d\cos\theta}$ for LL polarization and cm energy at at $M_{Z_2} = 620 \text{ GeV}$ and $M_{H^+} = 536.89 \text{ GeV}$ for tree level.

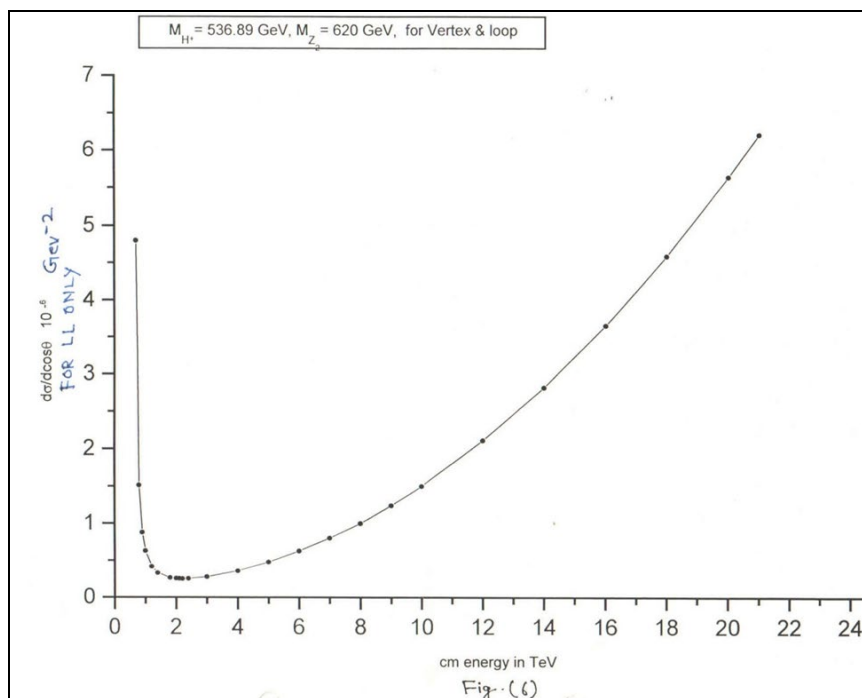


Fig 8: $\frac{d\sigma}{d\cos\theta}$ for LL polarization and cm energy at at $M_{Z_2} = 620 \text{ GeV}$ and $M_{H^+} = 536.89 \text{ GeV}$ for vertex and loop level.

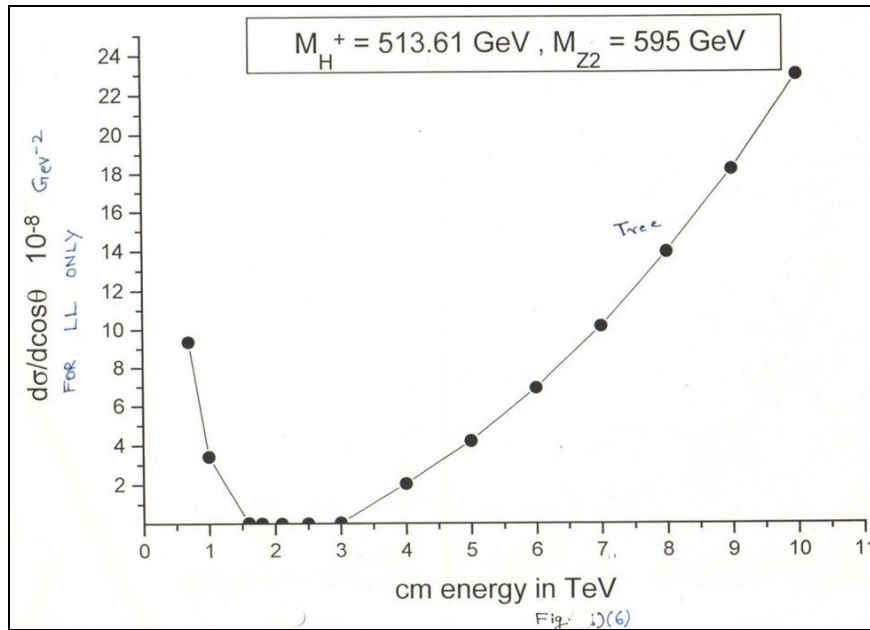


Fig 9: $\frac{d\sigma}{d\cos\theta}$ for LL polarization and cm energy at at $M_{Z_2} = 595 \text{ GeV}$ and $M_{H^+} = 513.61 \text{ GeV}$ for tree level.

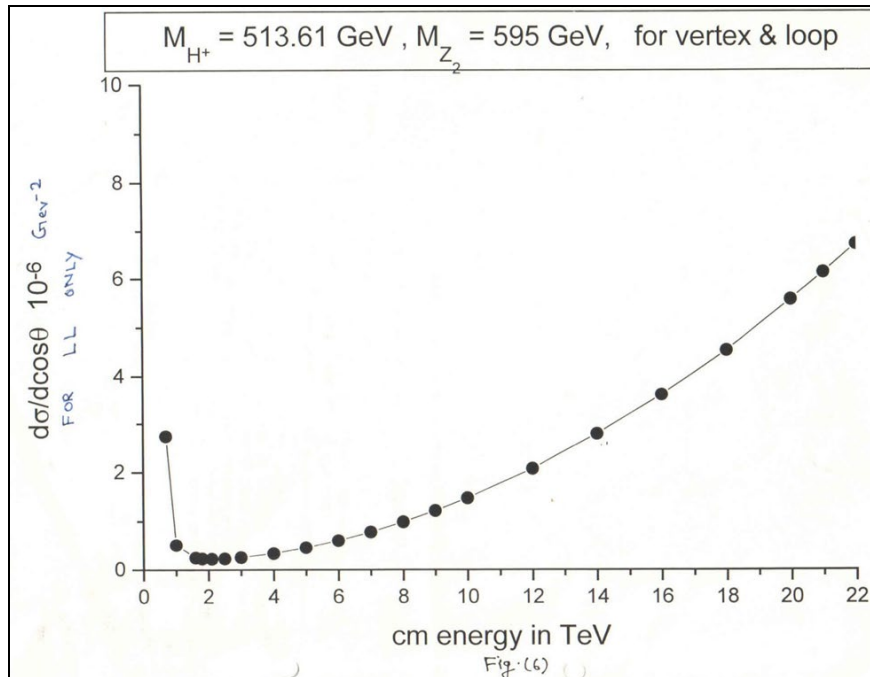


Fig 10: $\frac{d\sigma}{d\cos\theta}$ for LL polarization and cm energy at at $M_{Z_2} = 595 \text{ GeV}$ and $M_{H^+} = 513.61 \text{ GeV}$ for vertex and loop level.

Conclusion

- i). **Results [1,2] (Fig. 3 No. graph):** We are consider asymptotic case $\sqrt{s} = 0.5 \text{ TeV}$ and thereafter non-asymptotic case for gauge boson Z_1, Z_2 . Inclusion of form factor numerically in A_5 expression gives $\frac{d\sigma}{d\cos\theta}$, 2.5 to 0.5 in unit of 1R. This $\frac{d\sigma}{d\cos\theta}$ (1R) v/s TeV energy plot tells that it converges up to 2.1 TeV. This shows that there are not Unitarity violation. It can help to predict Z_2 at order of TeV energy linear collider.
- ii). **Results [1,2,5] (Fig. 4 No. graph):** A_5 is violating amplitude because it is proportional to cm energy s. So, we interested to look at the A_5 behavior with respect to CM-energy. We have plotted Σ_{LL} amplitude and shown that first this amplitude goes downward with minimum around 2100 GeV energy thereafter it increases rapidly. Such type of behavior has been observed for non-asymptotic case. Such type of behavior has been observed for non-asymptotic case. There should be some additional loop corrections diagrams that can stop rising part of A_5 after 2.1 TeV energies. In this regards the work is ongoing for further completion. This prediction is useful to separate Z_2 mass which violates delayed Unitarity [2].

iii). **Results [1,2,5] (Fig. 5,6 No. graph):** We have considered Superstring Inspired Extra U(1) model this provides physics beyond Standard model(SM), where we have studied form factors. These form factors achieve some constant values around 2.1 TeV and thereafter becomes constant. This result matches with present S, T values and form factors analysis which are called universal correction parameters. They do not change much, when CM energy increases. Therefore this result is strongly favoured. It suggested that this prediction could possibly be tested in the ending TESLA Collider at CERN. The result is favoured its present day analysis or particle Data for S, T and U values parameters and form factors values [6]. For cross section calculation we have found $\frac{d\sigma}{d\cos\theta}$, that it first falls to a minimum at 2.1 TeV energy and thereafter starts rising leading to Non-delayed Unitarity Violation. The predictions could possibly be tested in the ensuing TESLA collider (CERN).

References

1. Sahu RS *et al.*, XVDAE Symposium on HEP, Dept. of Physics, Univ. of Jammu, Jammu. 11-15 Nov., 2002, P76.
2. Sahu RS *et al.*, XVDAE Symposium on HEP, Dept. of Physics, Univ. of Jammu, Jammu. 11-15 Nov., 2002, P81.
3. Ahn C, Peskin ME, Nucl. Phys. B309, (1988) 221-258.
4. Sahu RS *et al.* Pramana Jr. of Phy., Vol. 52(No. 2), 145-175(1999) and Ph.D Thesis page 271, Univ. of Rajasthan, Jaipur (2000).
5. "Delayed unitarity in Extra U(1) model", R. S. Sahu, Pramana Jr of Phy. To be communicated 2023.
6. Phys. Rev. D Particle and field, Reviews, Tables & Plots (2022), R. L. Workman *et al.* (Particle Data Group), prog. Theor. Exp. Phys. 2022, 083C01 (2022). Bertram Schwarzschild, Physics, 2002, 66, <https://doi.org/10.1063/1.1381094>.